

# Revisiting the U-238 Thermal Capture Cross Section and Gamma-ray Emission Probabilities from Np-239 Decay

A. Trkov<sup>1\*</sup>, G. L. Molnár<sup>2†</sup>, Zs. Révay<sup>2</sup>, S. F. Mughabghab<sup>3</sup>, R. B. Firestone<sup>4</sup>,  
V. G. Pronyaev<sup>1</sup>, A. L. Nichols<sup>1</sup>, M. C. Moxon<sup>5</sup>

<sup>1</sup> Nuclear Data Section  
Department of Nuclear Sciences and  
Applications  
International Atomic Energy Agency  
Wagramerstrasse 5  
PO Box 100  
A-1400 Vienna  
Austria

<sup>2</sup> Institute of Isotopes  
Chemical Research Center  
Hungarian Academy of Sciences  
PO Box 77  
H-1525 Budapest  
Hungary

<sup>3</sup> National Nuclear Data Center  
Building 197D  
Brookhaven National Laboratory  
PO Box 5000  
Upton, NY 11973-5000  
USA

<sup>4</sup> Isotopes Project  
Building 88, MS-88R0192  
Lawrence Berkeley National Laboratory  
University of California  
1 Cyclotron Road  
Berkeley, CA 94720  
USA

<sup>5</sup> 3 Hyde Copse,  
Marcham,  
Abingdon  
Oxfordshire OX13 6PT  
England, UK

\* Corresponding author. Tel: +43-1-2600-21712; fax +43-1-26007.  
E-mail address: [a.trkov@iaea.org](mailto:a.trkov@iaea.org)

† Deceased

Total number of pages 36, including tables and figures: No. of Tables: 9, No. of Figures: 1.

## ABSTRACT

The precise value of the thermal capture cross section of  $^{238}\text{U}$  is uncertain, and evaluated cross sections from various sources differ by more than their assigned uncertainties. A number of the original publications have been reviewed to assess the discrepant data, corrections were made for more recent standard cross sections and other constants, and one new measurement was analyzed. Due to the strong correlations in activation measurements, the gamma-ray emission probabilities from the  $\beta^-$  decay of  $^{239}\text{Np}$  were also analyzed. As a result of the analysis, a value of  $2.683 \pm 0.012$  barns was derived for the thermal capture cross section of  $^{238}\text{U}$ . A new evaluation of the gamma-ray emission probabilities from  $^{239}\text{Np}$  decay was also undertaken.

## I. INTRODUCTION

Cross section databases have to be regularly improved in order to enhance further the predictive power of computational methods for reactor analysis and design. Clearly, the results are highly sensitive to the data adopted for the main uranium isotopes. One of the important recent changes entered into the ENDF/B-VI library since Release 5 has been an increase of the capture to fission ratio of  $^{235}\text{U}$  in the epithermal energy range [1]. This modification has improved the reactivity prediction in calculations for fast reactors, but caused under-predictions of reactivity in thermal lattices. Obviously, the previously low value for the epithermal capture of  $^{235}\text{U}$  compensated for an error in one or more of the other parameters, which still need to be identified. The thermal capture cross section of  $^{238}\text{U}$  is an obvious candidate for consideration. Within the Working Party on Evaluation Co-operation (WPEC), Subgroup 22 has been set up to address the problem [2]. The function of the subgroup is primarily to co-ordinate activities and to exchange information, while the actual work is supported by national projects and other sources. Measurements of the thermal capture cross section of  $^{238}\text{U}$  are reviewed in the present work.

Several measurements of the thermal neutron capture cross section can be found in the literature. They are summarised in Table I, which is based on information circulated within WPEC Subgroup 22. The weighted mean of the published data is  $2.705 \pm 0.010$  b, with a chi-square per degree of freedom of 0.66 that is lower than the expected value of  $1 \pm 0.27$  (two standard deviations for 18 measurements). This chi-squared value may indicate either the uncertainties assigned by the authors are too large, or that there is underestimation/omission of important correlations between different measurements. The compilation of recommended

thermal cross sections and resonance integrals by Mughabghab has remained unchanged for  $^{238}\text{U}$  in recent updates [21], and favours the Poenitz *et al* measurement of  $2.680 \pm 0.019$  barns [17]. The recommended cross section for the ENDF/B-VI library is 2.709 barns [1], and is remarkably close to the weighted average over all measurements, which is dominated by the Poenitz and Bigham measurements that claim the lowest uncertainty. None of the quoted references in the ENDF/B-VI files explain adequately how this value was deduced. The actual value in the evaluated nuclear data file ENDF/B-VI, Release 8 is 2.718 barns [1]. Some of the original publications describing experimental measurements have been reviewed in the present work to explore the discrepancies and eliminate differences due to the use of obsolete nuclear structure, decay and standard cross section data.

## II. RE-ANALYSIS OF EXISTING MEASUREMENTS

### *II.A. Thermal capture cross section measurements*

The experimental and analytical details found in many of the old publications are insufficient to allow a thorough re-analysis of the data. A more detailed review of some of the measurements (identified by the lead author) is given below, with the aim of selecting a set of reliable measurements to estimate the average capture cross section of  $^{238}\text{U}$ .

Whenever possible, the parameters reported in the papers have been converted to the original measured quantities (for example, measured cross section ratios) in order to treat the correlations explicitly. Renormalization to more recent standards was carried out where appropriate. The selected measurements were fitted simultaneously, as described later.

*Rajput and MacMahon* [19]: Measurements of the thermal cross section and resonance integral are reported using a calibrated pure germanium detector to monitor the 74.7 keV gamma-ray line from the 23 minutes  $\beta^-$  decay of  $^{239}\text{U}$ . Gold is used as the standard at thermal energies. Together with cobalt, manganese and zinc, gold is also used to measure the relative magnitude and shape of the epithermal flux. The authors do not quote the values of the standard cross sections used. The thermal to resonance integral ratio is only  $\sim 18.8$ , which results in a large uncertainty due to a strong correction for epithermal spectrum.

Although the most recent measurement published in the open literature, this study does not meet the required quality standards, and was excluded from the final selection of measurements for further analysis.

*De Corte et al* [18, 25]: The directly measured quantity in the experimental determination of  $k_0$  factors for activation analysis is the ratio of specific activities producing characteristic gamma rays with energy  $E_\gamma$ , corrected for the epithermal flux contribution. Parameter  $k_0$  expressed in terms of the basic physical constants is defined by:

$$k_0 = \frac{\theta_x g_x \sigma_{0x} P_{\gamma x}}{\theta_s g_s \sigma_{0s} P_{\gamma s}} \frac{M_s}{M_x} \quad (1)$$

where:

$\theta$  is the natural abundance of the isotope,

$g$  is the effective g-factor of the isotope to account for non-1/v cross sections,

$\sigma_0$  2200 m/s capture cross section value of the isotope,

$P_\gamma$  emission probability of a gamma ray with energy  $E_\gamma$ ,

$M$  molar mass of the element,

$x$  index referring to the measured element,

$s$  index referring to the standard.

Measured  $k_0$  factors were converted to the ratios of the isotopic partial gamma-production cross sections in order to simplify the analysis:

$$R_\gamma = \frac{P_{\gamma x} \sigma_{0x}}{P_{\gamma s} \sigma_{0s}} = k_0 \frac{\theta_s g_s M_x}{\theta_x g_x M_s}. \quad (2)$$

The measured  $k_0$  factors and partial cross section ratios  $R_\gamma$  for several gamma lines are given in Table II. The natural abundances of  $^{197}\text{Au}$  and  $^{238}\text{U}$  are 100% and 99.2745%, respectively [22], and the corresponding g-factors were 1.005 for  $^{197}\text{Au}$  and 1.002 for  $^{238}\text{U}$  [21]. The molar masses of gold and uranium were 196.96655 [g] and 238.02891 [g], respectively [23]. The relative uncertainties in the ratios  $R_\gamma$  are the same as the uncertainties in the  $k_0$  factors, because the uncertainties in the abundances and molar masses are negligible. The deviation of the g-factors from unity is also small, so that the errors in the g-factors do not influence the ratios.

According to the authors, the reported  $k_0$  factors were determined by averaging a large number of measurements performed on different irradiation facilities. The uncertainty is therefore statistical. Systematic uncertainty comes from the uncertainty in the half-lives of  $^{198}\text{Au}$  and  $^{239}\text{Np}$  (which is small), detector calibration and the correction procedure for epithermal neutrons. This correlated uncertainty is estimated to sum to 0.5%, and is added later (square root of the sum of squares) to the total uncertainty.

The  $k_0$  factor for the 228.1-keV gamma ray is quoted to be the sum of the 226.4- and 228.1-keV line contributions. The 227.8-keV gamma ray that is listed in the latest evaluation of Browne [24] is not mentioned due to the uncertainty of its existence. Therefore, the sum of the gamma rays with energies between 226 and 228

keV was used as the fitted parameter in order to avoid ambiguity and allow formal consistency with other measurements using detectors of different resolution powers.

The value of the  $k_0$  factor for the 228.1-keV gamma ray is taken from reference [25]. A difference of 0.4% in the quoted value compared to that in the older reference [18] is due to the small fission product interference correction. The correction procedure seems justified [26], but is not exact, and therefore the uncertainty of the  $k_0$  factor for the 228.1-keV gamma ray has been increased by 0.4%.

The  $k_0$  factor for the 106.1-keV gamma ray is also taken from reference [25]. Renormalized to the 228.1-keV value, this factor does not represent an independent measurement, therefore it has been effectively excluded from the analysis by adding 20% to the uncertainty.

No uncertainty is quoted for the 285.5-keV gamma ray, and the influence of this emission was minimised by assigning 50% uncertainty to the ratio.

The ratios  $R_\gamma$  in Table II are the input parameters for the simultaneous least squares analysis.

*Poenitz et al* [17]: This measurement appears to be independent of any assumption about the gamma-ray emission probabilities of  $^{239}\text{Np}$  because the detector is calibrated by means of an  $^{243}\text{Am}$  source that decays to  $^{239}\text{Np}$ , which is also the nuclide measured after neutron capture in  $^{238}\text{U}$  and the subsequent beta decay of  $^{239}\text{U}$ . The cross section of the gold standard has not changed since this measurement was published. There is a small change to the recommended half-life of  $^{239}\text{Np}$  from 2.355 days to 2.3565 days, but the effect of this change is negligible. The 277.7-keV gamma ray alone was used in the determination of the thermal cross section. The published value of  $2.680 \pm 0.019$  barns is converted to the ratio with the cross section of gold that is quoted to be  $98.65 \pm 0.30$  barns in the original paper:

$$R_\sigma = \frac{\sigma_0(^{238}U)}{\sigma_0(^{197}Au)} = 0.02717 \pm 0.64\%$$

This ratio is the fitted parameter in the simultaneous least squares analysis. The relative uncertainty in the cross section of gold is subtracted from the quoted uncertainty in the  $^{238}\text{U}$  cross section (square root of the difference of squares) to define the uncertainty of the ratio.

*Bigham et al* [16]: This study is a measurement of the neutron capture in  $^{238}\text{U}$  relative to the fission in  $^{235}\text{U}$  in samples of “natural” uranium, and like *Poenitz et al* measurement uses an  $^{243}\text{Am}$  source to calibrate the gamma-ray detector. As revealed by the contents of the original paper, accurate measurements were carried out that included the decay schemes, the effective temperature of the neutron flux, the cadmium ratio and several other quantities.

Corrections were made in the present work to account for more recent data for the decay constants, thermal g-factors and cross sections for  $^{235}\text{U}$ ; these affected quantities are listed in Table III. Substitution of the updated parameters increases the measured value to 2.751 barns.

The authors do not appear to have checked the  $^{235}\text{U}$  content of their “natural” uranium sample. The spread in the  $^{235}\text{U}$  content of uranium from ores is at most  $\pm 0.6\%$ , but present day samples can contain uranium from depleted and irradiated sources, all of which will have varying  $^{235}\text{U}$  content. In this measurement, the uncertainty in the abundance of  $^{235}\text{U}$  directly affects the result.

The dead time losses for the fission measurements are quoted as between 0.1 and 0.7% when using a 0.5- $\mu\text{s}$  time constant in the amplifier. However, there is no mention of any dead time corrections for the gamma-ray detector and associated electronics. A  $\sim 2 \mu\text{s}$  pulse shaping time constant was used which would indicate a

dead time of between 5 and 10  $\mu$ s. Only if the gamma-ray count rates from the  $^{243}\text{Am}$  source and the decay of the  $^{239}\text{Np}$  from the capture in  $^{238}\text{U}$  were very similar, would the corrections cancel one another.

The effective efficiency of the alpha/fission counter is assumed to be the same for alphas from the Am source and the fission fragments from the uranium samples (i.e., absorption in the two source foils and the detector materials for alphas and fission fragments are the same). This may not be the case, considering the required accuracy of the final result.

There is no comment about the  $\sim 0.75\%$  decrease in values  $[\gamma^1(\text{U})/\gamma(\text{Am})]/F(\text{U})$  with increasing sample thickness, given in column 3 of Table II in the paper by Bigham *et al* [16]. The implications of this trend are not known.

The  $^{239}\text{Np}$  activity was determined from the count rate around the 106.1-keV gamma-ray line, which could not be resolved completely from the plutonium X-rays at 103.8-keV  $K_{\alpha 1}$  and 99.6-keV  $K_{\alpha 2}$  with the equipment used. In fact, the sum of the three peaks was assumed to be representative of the  $^{239}\text{Np}$  activity in the irradiated uranium sample, as well as in the americium sample used for calibration.  $^{242}\text{Cm}$  and  $^{244}\text{Cm}$  are present in the Am sample, and they both decay by alpha emission into isotopes of plutonium. The contribution of Pu isotopes was checked for the  $\alpha$  spectra, but is not mentioned for the  $\gamma$  spectra. Pu isotopes also contribute to the intensity of the X-ray lines, to give a constant background to the  $^{243}\text{Am}$  count rate that is not present in the measurement of the  $^{239}\text{Np}$  decay. The subtraction of such a background would cause a further increase in the observed cross section. Measurements by Bresesti *et al* [28] of the emitted gamma-ray spectra from various irradiated uranium samples show a very complex spectrum in the energy region around 106 keV. Other experimentalists have avoided using the 106.1-keV line due to the interference of the

plutonium X-ray lines. There is no mention of any measurements of the X- and gamma-ray emissions from the samples prior to irradiation or at times when activity from the  $^{239}\text{Np}$  was negligible.

Hunt *et al* [15] noted that Axton *et al* [29] questioned the accuracy of the fixed geometry counting system used to determine the neutron flux. Perhaps this criticism is not valid as Axton *et al* [29] describe a  $2 \times 2\pi$  fission fragment detector, whereas Bigham *et al* detector has a small solid angle ( $\sim 4\pi/150$ ) normal to the sample.

For reasons stated above, this measurement is excluded from further consideration.

*Hunt et al* [15]: The main uncertainty in the measurement is the assumed decay scheme of  $^{239}\text{U}$  and the branching ratios for different beta particles. The beta counter used in this measurement had an effective efficiency that depended on the beta energy, the thickness of both the sample and cover. Detector calibration was undertaken assuming that low-energy beta particles were undetected ( $\sim 0.5\%$ ), and an 80/20 ratio for the 1211- and 1285-keV beta particles. An overall efficiency of 70% for the 1211- and 1285-keV betas for a ratio of 80/20 is quoted in the paper. The more recently evaluated decay scheme is shown in Table IV [24]. A higher fraction of low-energy beta particles is more easily absorbed in the sample and could lower the detection efficiency. Dean has carried out a calculation, assuming that the two strong beta emissions are allowed transitions [30]. He found that an effective low-energy cut-off at 265 keV was required to give an efficiency of 70% for the two betas. This cut-off was then applied in a calculation of the efficiency for the present beta-decay scheme of  $^{239}\text{U}$ , including the beta emissions of smaller intensity but with the same maximum beta energies for the two strongest transitions. He concluded that

the more detailed decay scheme does not cause any significant change in detector efficiency.

The difference in the half-life of  $^{239}\text{U}$  introduces negligible error (quoted to be 2.35 days compared with the modern value of 2.3565 days).

The value of the g-factor that accounts for the deviation from the  $1/v$  cross-section behaviour does not affect the results significantly (quoted to be 1.0023 compared with 1.002 used in this work, based on ENDF/B-VI, Release 8 data).

The quoted cross section of the gold standard of  $98.8 \pm 0.3$  barns is used to reconstruct the ratio  $R_\sigma$  which was actually measured. The relative uncertainty in the cross section of gold is subtracted (square root of the difference of squares) to derive the uncertainty of the ratio:

$$R_\sigma = \frac{\sigma_0(^{238}\text{U})}{\sigma_0(^{197}\text{Au})} = 0.02725 \pm 1.58\%$$

This ratio is the fitted parameter in the least squares analysis, which explicitly takes into account the correlation with the cross section of gold.

*Transmission measurements:*  $^{238}\text{U}$  is an even-even nucleus and there is virtually no scattering contribution to the total cross-section at neutron energies below the first Bragg edge ( $\sim 2.3$  meV). Transmission measurements by the time-of-flight method carried out below 2.3 meV can be extrapolated to 0.0253 eV assuming  $1/v$  dependence of the cross section. The measured values do not depend on any standard, decay schemes or effective temperature of the neutron flux. However, there is the need to correct for the deviation from  $1/v$  dependence. The purity of the sample is also important as any impurity with a cross-section of  $\sim 1000$  b need only be present at a level of 10 ppm to give an increase in the observed extrapolated cross section of 0.01 b.

There are three published values of the thermal capture cross section of  $^{238}\text{U}$  derived from low-energy transmission measurements. Capture cross sections at 2.3 meV and 0.0253 eV in the ENDF/B-VI.8 library indicate a correction of 0.010 barns for the deviation from  $1/\nu$  behaviour. Two of the transmission measurements are included in the final selection [11, 13], while an earlier measurement by Egelstaff [8] is excluded because of the large correction due to the  $^{235}\text{U}$  content of the natural uranium samples.

The transmission measurement by Cocking and Egelstaff [12] was measured relative to the gold standard (assuming a cross section of  $98.6 \pm 0.7$  barns) in a bismuth-filtered neutron beam with an effective temperature of 14K. The reported cross section of  $2.69 \pm 0.04$  barns was converted to the ratio that was measured ( $R_m$ ) by dividing by the quoted cross section of gold, since the authors assumed  $1/\nu$  dependence of the cross sections. The measured ratio is:

$$R_m = \frac{\sigma_0(^{238}\text{U})}{\sigma_0(^{197}\text{Au})} \frac{g(^{238}\text{U}, 14\text{K})}{g(^{197}\text{Au}, 14\text{K})} \quad (3)$$

where the g-factors correspond to the effective temperature 14K. The fitted parameters is the cross section ratio:

$$R_\sigma = \frac{\sigma_0(^{238}\text{U})}{\sigma_0(^{197}\text{Au})} = R_m \frac{g(^{197}\text{Au}, 14\text{K})}{g(^{238}\text{U}, 14\text{K})} = 0.02714 \pm 1.5\%$$

The g-factor ratio for correcting the measured ratio is calculated from ENDF/B-VI, Release 8 data, and amounts to 0.9949. The relative uncertainty of this ratio is calculated by removing the contribution of the standard (square root of the difference of squares) and adding 0.2% to take into account the uncertainty of the g-factors.

*Other measurements:* The measurements of Halperin *et al* [14] refer to the determination of the effective reactor cross sections, and were not optimised for the

highly accurate determination of basic cross section data for individual nuclides. No further consideration is given to these data.

The main problem with the old activation and pile oscillator measurements is that most reports do not mention details of the corrections for the epithermal flux. A cadmium ratio of  $\sim 10000$  to 1 is required in order to make the epithermal flux contribution smaller than 1%. The pile oscillator measurements also require very pure samples of  $^{238}\text{U}$  or detailed notes about the correction for any impurities. Due to insufficient information about various corrections, the old measurements not discussed explicitly above are excluded from further consideration.

### *II.B. Gamma-ray emission probability measurements*

Due to strong correlation with the activation measurements, the gamma-ray emission probability measurements have been explicitly included as fitted parameters in the simultaneous least squares analysis instead of adopting the recently evaluated values of Browne [24]. Fitted gamma-ray emission probabilities are thus obtained as a by-product, based on a much broader experimental database than used by Browne and treating many of the correlations explicitly.

The measured gamma-ray emission probabilities are shown in Table V. High-resolution gamma-ray spectrometers were used in the more recent measurements by Woods *et al* [31], Vaininbroukx *et al* [32] and Ahmad [33], and the two peaks in the gamma-ray spectra at 226.4 and 228.2 keV could be partly resolved. Diagrams of the measured spectra in older measurements reveal that the resolution was poor. Starozhukov *et al* [34] attempted to resolve the 226.4- and 228.2-keV peaks, while in their older measurement Ahmad and Wahlgren [35] quoted a value for the sum of the two emissions.

As described for the De Corte measurement, the emission probabilities of gamma rays with energies between 226 and 228 keV were summed and treated as a single-fitted parameter to avoid ambiguity about the existence of the gamma line at 227.8 keV, and to allow objective treatment of the measurements with lower resolution detectors.

With the low-resolution detector in the older measurement of Ahmad and Wahlgren, the X-rays around the 106.1-keV peak could not be resolved, and the authors did not attempt to make a correction. The weight of the measurement intensity of the 106.1-keV gamma ray in the old measurement of Ahmad and Wahlgren was minimised by adding 20% to the uncertainty.

Emission probabilities for different gamma rays derived from the same measurement have common systematic errors originating from the assumed half-lives, detector calibration, etc. This systematic error was assumed to be included in the uncertainty of the quoted emission probabilities of individual gamma rays, but a 0.5% correlated uncertainty was assigned between the emission probabilities at different energies.

Another measurement of the emission probability of the 277.6-keV gamma ray by Yurova *et al* [37] appears in the literature. By careful reading of this paper, the measured gamma-ray emission probability of  $14.1 \pm 0.4\%$  was judged to be a partial gamma-production cross-section measurement relative to the gold standard, assuming  $^{238}\text{U}$  thermal capture cross section of  $2.68 \pm 0.03$  barns. The write-up is rather sketchy: does not specify the adopted gold cross section, the composition of the sample, or details of the applied corrections. The measurement was converted to the partial gamma-production cross section, where the measured  $P_\gamma$  is expressed as a fraction multiplied by the quoted thermal capture cross section:

$$P_\gamma(277.6 \text{ keV}) \sigma_0 = 0.3779 \pm 0.0099 \text{ barns}$$

The uncertainty due to the  $^{238}\text{U}$  thermal capture cross section was subtracted (square root of the difference of squares or relative uncertainties), but due to the uncertainty concerning the cross section of gold and the other parameters, 1% was added to the total relative uncertainty. For practical reasons the actual fitted parameter was the product:

$$P_\gamma(277.1 \text{ keV}) \sigma_0 = 37.79 \% \text{ barns} \pm 3.9 \%$$

with  $P_\gamma$  expressed as %, and the relative uncertainty expressed as % of [% barns].

### III. EXTENDED ANALYSIS OF NEW MEASUREMENTS

The partial elemental gamma-ray production cross section of uranium has been measured in Budapest and published recently [38]. These data originate from a careful activation measurement on natural uranium acetate samples in a cold neutron beam facility. The chopper installed on the facility enables pulsed operation so that prompt and delayed gamma-ray spectra can be measured simultaneously. This arrangement permits normalisation to the hydrogen standard, which is homogeneously mixed with uranium in a precisely defined ratio based on the known stoichiometry of uranium acetate. The hydrogen counts were determined from the prompt spectrum, while the  $^{239}\text{Np}$  peaks were obtained from the decay spectra measured in the same geometry following 1, 4 and 9-days cooling time after irradiation.

While only the partial cross section of  $0.382 \pm 0.006$  barns for the 277.7-keV gamma ray was reported in Ref. [38], the measured spectra have subsequently been re-analysed in order to determine the partial cross sections for as many strong gamma rays originating from the beta decay of  $^{239}\text{Np}$  as possible. The present analysis of the

measurements differs from the preliminary study [38] with respect to small improvements in the peak area determination, averaging of the measurements at three cooling times, and explicit treatment of  $^{239}\text{U}$  decay.

Only the measured 228.2-keV gamma rays were found to be sensitive to interference from fission product gamma-ray emissions: the partial cross section measured from this gamma ray increased with cooling time, and exceeded the 1-day value by 6% after 4-days cooling, and by 30% after 9-days cooling; hence, this gamma ray has been excluded from the analysis. The 106.1-keV gamma rays were well separated from the 103.7-keV Pu X-rays in all three decay measurements. Self-absorption in the target was about 2% at this energy, and this effect could be easily corrected.

The quoted experimental uncertainty includes the uncertainty in determining the net areas of the measured gamma-ray peaks and the relative detection efficiencies. There is a systematic uncertainty that arises from uncertainties in the decay constants of the  $^{239}\text{U}$  capture product and daughter  $^{239}\text{Np}$ , and the beta feedings in the decay of  $^{239}\text{U}$  and  $^{239}\text{Np}$  ( $^{239}\text{U}$  decays to  $^{239}\text{Np}$  with a short half-life that required 0.7% correction of the measured activity in the present study). However, the half-life of  $^{239}\text{Np}$  is known with high precision, and therefore the uncertainty in the measured data can be realistically estimated.

Original experimental results were quoted as elemental partial gamma production cross sections:

$$\sigma_\gamma = \theta_x g_x \sigma_{0x} P_{\gamma x} \quad (4)$$

while the quantities actually measured were the ratios of specific activities of the gamma rays from  $^{239}\text{Np}$  decay and the 2223-keV prompt gamma ray from deuterium

after neutron capture in hydrogen. The latter parameter is the standard in which the stoichiometric ratio  $S_H$  of H:U atoms is taken into account:

$$k_{0(\gamma)} = \frac{A_{x(g)}}{A_s} \frac{1}{S_H} = \frac{\theta_x g_x \sigma_{0x} P_{\gamma x}}{\theta_s g_s \sigma_{0s} P_{\gamma s}} \frac{M_s}{M_x} \quad (5)$$

As in the case of the measurements by De Corte and Simonits [18], the fitted parameters are isotopic partial gamma-production cross section ratios:

$$R_\gamma = \frac{P_{\gamma x} \sigma_{0x}}{P_{\gamma s} \sigma_{0s}} = \frac{\sigma_\gamma(U)}{\sigma_\gamma(H)} \frac{\theta(H)}{\theta(^{238}U)} \frac{g(H)}{g(^{238}U)} \frac{S_H^*}{S_H} \quad (6)$$

where the isotopic partial gamma production cross section of hydrogen is calculated from the thermal cross section  $\sigma_{0s}(H) = 0.3326 \pm 0.0007$  barns with  $P_{\gamma s} = 100\%$  gamma-ray emission probability; the abundances are  $\theta(^{238}U) = 99.2745\%$  and  $\theta(^1H) = 99.9885\%$  [22]. The relative uncertainty of the ratio is equal to the relative uncertainty of the partial elemental gamma production cross section, since the uncertainties of the other components are small.

The ratio of the  $g$ -factors was calculated using cross section curves from the ENDF/B-VI.8 library and the spectrum  $\phi(E)$  from the cold neutron beam facility in Budapest as measured by the time-of-flight technique [20]:

$$\frac{g(^{238}U)}{g(^1H)} = \frac{\sigma_0(^1H) \int \sigma_{U^{238}}(E) \phi(E) dE}{\sigma_0(^{238}U) \int \sigma_{H1}(E) \phi(E) dE} \quad (7)$$

The ratio  $g(^{238}U)/g(^1H)$  was found to be 0.997. Since  $g$ -factors do not depend on the absolute accuracy of the cross section but only on the shape and the  $g$ -factor ratio is very close to one, the error introduced by the calculated  $g$ -factor ratio is considered to be negligible.

The quoted elemental partial gamma-production cross sections were based on the assumption of an ideal stoichiometry of uranium acetate with two water

molecules per each molecule of the acetate, giving H:U ratio  $S_H^* = 10$ . An acetate sample of about 1 g was weighed, heated to 120°C (which is well below the decomposition temperature) to expel the lattice water, and weighed again. From the difference in weights the H:U ratio  $S_H = 10.07$  was determined. This correction for stoichiometry was taken into account when calculating the isotopic partial cross section ratios; 0.7% uncertainty was added to the measured values to account for the uncertainty in stoichiometry.

The measured elemental partial gamma-production cross sections for gamma rays of different energies and the corresponding isotopic partial gamma-production cross section ratios to hydrogen standard are listed in Table VI. The ratios are the fitted parameters in the simultaneous least squares analysis.

#### IV. LEAST SQUARES ANALYSIS

The least squares fitting procedure was performed with the ZOTT99 code [39], using the option to convert all input parameters and uncertainties automatically to the log-domain. Working in the log-domain is more appropriate for evaluations that involve ratios and products because this approach causes a non-linear evaluation problem to be converted into a linear one. For example, if  $c$  is a measured quantity and  $a$  and  $b$  are parameters to be estimated, the model relation  $c = b/a$  is non-linear in  $a$ , but the equivalent relation  $\log(c) = \log(b) - \log(a)$  is precisely linear in both  $\log(a)$  and  $\log(b)$ .

Input parameters (i.e., standards known with a relatively high precision that are not expected to change as a result of the fitting procedure) and initial values for the fitted parameters (non-informative priors, which do not affect the final result) are given in Table VII.

Experimental data as entered into the fitting procedure are listed in Table VIII. The uncertainties are the relative total uncertainties (expressed as %), except for the data of De Corte and Simonits [18], to which a 0.5% correlated error is added. The correlated errors for all other measurements are also listed in this table.

The ZOTT99 code was allowed to identify outlying data and increase their variance iteratively until  $\chi^2$  dropped below 1. Only the measurement of the emission probability of the 106.1-keV gamma ray by Vaninbroukx *et al* was identified as the outlier [32].

The relative differences of the measured data listed in Table VIII from the final fitted results are shown in Figure 1, in which the error bars correspond to the relative uncertainties in the measured data.

Interpretation of the results of a statistical analysis is often difficult because of the inherent assumptions and approximations about statistical and systematic uncertainties and their correlations. Under such circumstances and to gain confidence in the results, a sensitivity study was carried out by selectively removing individual data entries from the fitting procedure through the arbitrary procedure of increasing their uncertainty by 50%. The influence of the removal of selected data entries on the thermal capture cross section and the 106.1-keV gamma-ray emission probability is presented in Table IX. The results demonstrate that no single entry dominates the overall result, and that the ZOTT99 procedure of identifying and treating outliers is justified.

## V. CONCLUSIONS

Several sets of  $^{238}\text{U}$  thermal capture cross-section measurements from the literature were reviewed. Measurements that did not meet the quality standards or for

which there was insufficient information available were discarded from further consideration. Thermal capture cross sections of  $^{238}\text{U}$  by Poenitz *et al* [17], Hunt *et al* [15], De Corte *et al* [18, 25] and Molnár *et al* [38] were processed, introducing corrections for more recent data as necessary. The transmission measurements of Palevsky *et al* [11], Cocking and Egelstaff [12] and Egelstaff and Hall [13] were also considered. Due to the strong correlation with the partial cross section measurements the gamma-ray emission probability measurements by Woods *et al* [31], Vaninbroukx *et al* [32], Ahmad [33, 35], Starozhukov *et al* [34] and Mozhaev *et al* [36] were included in the analysis. The measurement by Yurova *et al* [37] was included as a partial gamma-ray production cross section.

The data were analysed with the ZOTT99 least squares fitting code. Experimental data show good consistency. The least squares fitting procedure identified a single outlier, namely the 106.1-keV gamma-ray emission probability measured by Vaninbroukx *et al* [32]. Increasing the uncertainty in this measurement by a factor of approximately two brought the  $\chi^2$  below one. Therefore, the emission probability of the 106.1-keV gamma ray was determined mainly from the measurements of Woods *et al* [31] and Molnár *et al* [38]; both are measured with high-resolution spectrometers and exhibit good consistency, so we believe they provide a reasonably reliable estimate of the true gamma-ray emission probability.

The final fitted thermal capture cross section of  $^{238}\text{U}$  is:

$$\sigma_0(^{238}\text{U}) = 2.683 \pm 0.012 \text{ barns.}$$

Excluding the  $P_\gamma(106.1 \text{ keV})$  value of Vaninbroukx *et al* has no effect on the fitted thermal capture cross section of  $^{238}\text{U}$  and gives  $\chi^2$  per degree of freedom of 0.854. The relatively low  $\chi^2$  per degree of freedom may be an indication that either the variances of the experimental data are overestimated, or the correlations representing

the common uncertainties of the experimental data are underestimated. As shown in Table IX, no single experiment dominates the result, which varies by only 0.1% when the values of individual authors are eliminated. We believe that any re-analysis of the covariance matrices of the experimental data (i.e., increasing individual elements of the covariance matrices of evaluated data) will not affect the evaluated values in the fit, due to the insensitivity of the evaluated values to the results of individual authors.

Recommended gamma-ray emission probabilities (expressed in %) and their uncertainties were derived from this exercise:

$P_\gamma(106.1 \text{ keV})$	=	25.34	$\pm 0.17$
$P_\gamma(181.7 \text{ keV})$	=	0.0831	$\pm 0.0024$
$P_\gamma(209.8 \text{ keV})$	=	3.363	$\pm 0.020$
$P_\gamma(226-228 \text{ keV})$	=	11.499	$\pm 0.087$
$P_\gamma(254.4 \text{ keV})$	=	0.1092	$\pm 0.0022$
$P_\gamma(272.6 \text{ keV})$	=	0.0766	$\pm 0.0019$
$P_\gamma(277.6 \text{ keV})$	=	14.505	$\pm 0.079$
$P_\gamma(285.5 \text{ keV})$	=	0.7939	$\pm 0.0064$
$P_\gamma(315.9 \text{ keV})$	=	1.600	$\pm 0.012$
$P_\gamma(334.3 \text{ keV})$	=	2.056	$\pm 0.013$

The present analysis has important implications for new evaluations of the major actinides that are in progress in various national projects. The findings presented herein contribute to the reduction of the observed under-prediction of reactivity for thermal reactor lattices. The recommended gamma-ray emission probabilities as fitted also represent an improvement compared to the most recent evaluation, since a much larger experimental database has been included in the analysis that treats many of the correlations in the measurements.

The analysis does not entirely remove the need for a new measurement of the thermal capture cross section of  $^{238}\text{U}$ . Most of the measurements are relatively old,

and some important parameter may have been overlooked that affects the measurements. A new measurement with an accuracy much better than 1% would be beneficial to confirm the results of the present analysis.

## REFERENCES

- [1] Cross section evaluation working group, *ENDF/B-VI Summary Documentation*, BNL-NCS-17541 (ENDF-201) (1991), edited by P.F. Rose, National Nuclear Data Center, Brookhaven National Laboratory, Upton, NY, USA.
- [2] WPEC, Working Party on Evaluation Co-operation, Subgroup 22, OECD/NEA, Paris; <http://www.nea.fr/html/science/wpec/>.
- [3] H.L. ANDERSON, J. BISTLINE, J. DABBS, H. HESKETT, W. STRUM and J. TABIN, CP-2079, 4408 (1944).
- [4] W.E. GRUMITT, J. GUERON and G. WILKINSON, MC-70 44 (1944).
- [5] G.A. LINENBERGER and J.A. MISKEL, LA-467, 4601 (1946).
- [6] H. POMERANCE, “Thermal neutron capture cross sections of uranium”, ORNL-CF 52-4-15 (1952).
- [7] S. HARRIS, D. ROSE and H. SCHROEDER, “Thermal neutron absorption cross-section of  $U^{238}$ ”, ANL-5032, 7, (1953).
- [8] P.A. EGELSTAFF, “The neutron absorption cross sections of  $U^{238}$  and  $U^{235}$  at 2,200 m/sec.”, *J. Nucl. Energy*, **1** (1954/55) 92.
- [9] V. S. CROCKER, “The thermal neutron activation cross-sections of  $U^{238}$  and  $Th^{232}$ ”, *J. Nucl. Energy*, **1** (1954/55) 234.
- [10] V.G. SMALL, “The thermal neutron absorption cross-sections of  $U^{238}$  and  $Th^{232}$ ”, *J. Nucl. Energy*, **1** (1955) 319.
- [11] H. PALEVSKY, R.S. CARTER and D. HUGHES, Conf. Geneva 1955 147 (832).

- [12] S. COCKING and P.A. EGELSTAFF, “The neutron absorption cross sections of  $U^{238}$  and  $U^{235}$  at 2,200 m/sec.”, AERE Harwell, NRDC **84** part 2, 9; December 1955.
- [13] P.A. EGELSTAFF and J.W. HALL, AERE Harwell, NRDC **84** part 2, 9; December 1955.
- [14] J. HALPERIN, J.O. BLOOMEKE and D.A. MRKVICKA, “Effective reactor cross sections in MTR fuel assemblies”, *Nucl. Sci. Eng.*, **3** (1958) 395-402.
- [15] J.B. HUNT, J. C. ROBERTSON and T.B. RYVES, “A measurement of the thermal neutron radiative capture cross section of  $^{238}U$ ”, *J. Nucl. Energy*, **23** (1969) 705-711.
- [16] C.B. BIGHAM, R.W. DURHAM and J. UNGRIN, “A direct measurement of the thermal neutron conversion ratio of natural uranium”, *Can. J. Phys.*, **47** (1969) 1317.
- [17] W.P. POENITZ, L.R. FAWCETT Jr. and D.L. SMITH, “Measurements of the  $^{238}U(n, \gamma)$  cross section at thermal and fast neutron energies”, *Nucl. Sci. Eng.*, **78** (1981) 239-247.
- [18] F. DE CORTE and A. SIMONITS, “ $k_e$ -Measurements and related nuclear data compilation for  $(n, \gamma)$  reactor neutron activation analysis”, *J. Radioanal. Nucl. Chem.*, **133** (1989) 43-130.
- [19] M.U. RAJPUT and T.D. MACMAHON, “Measurements of thermal neutron cross section and resonance integrals of  $^{74}Se$ ,  $^{75}As$ ,  $^{94}Zr$ ,  $^{134}Cs$ ,  $^{238}U$ ”, *J. Radioanal. Nucl. Chem.*, **189** (1995) 51-58.

[20] G.L. MOLNÁR and Zs. RÉVAY, Institute of Isotopes, Chemical Research Center, Hungarian Academy of Sciences, Budapest, this work, April 2003.

[21] S.F. MUGHABGHAB, “Thermal neutron capture cross sections, resonance integrals and g-factors”, INDC(NDS)-440, February 2003.

[22] K.J.R. ROSMAN and P.D.P. TAYLOR, “Isotopic Compositions of the Elements – 1997”, *J. Phys. Chem. Ref. Data*, **27** (1998) 1275-1287.

[23] T.B. COPLEN, “Atomic Weights of the Elements 1999”, *J. Phys. Chem. Res.*, **30** (2001) 701-712.

[24] E. BROWNE, “Nuclear Data Sheets for A=235, 239” *Nucl. Data Sheets*, **98** (2003).

[25] F. DE CORTE, A. SIMONITS, F. BELLEMANS, M.C. FREITAS, S. JOVANOVIĆ, B. SMODIŠ, G. ERDTMANN, H. PETRI and A. DE WISPELAERE, “Recent advances in the  $k_0$ -standardization of neutron activation analysis: extensions, applications, prospects”, *J. Radioanal. Nucl. Chem.*, **169** (1993) 125-158.

[26] F. DE CORTE, “Problems and solutions in the standardization of reactor neutron activation analysis”, *J. Radioanal. Nucl. Chem.*, **160** (1992) 63-75.

[27] J.K. TULI, NNDC Wallet Cards, Brookhaven National Laboratory, (2000).

[28] A.M. BRESESTI, M. BRESESTI and H. NEUMANN, “A method for absolute determination of  $^{238}\text{U}$  capture rates”, *J. Nucl. Energy*, **23** (1969) 379-386.

- [29] E.J. AXTON, A.G. BARDELL and B.N. AUDRIC, “A technique for the absolute counting of nuclear fission events”, *J. Nucl. Energy*, **23** (1969) 457-468.
- [30] C.J. DEAN, Serco Group plc., UK, private communication, September 2003.
- [31] S.A. WOODS, D.H. WOODS, M.J. WOODS, S.M. JEROME, M. BURKE, N.E. BOWLES, S.E.M. LUCAS and C. PATON WALSH, “Standardisation and measurement of the decay scheme data of  $^{243}\text{Am}$  and  $^{239}\text{Np}$ ”, *Nucl. Instrum. Meth. Phys. Res.*, **A369** (1996) 472-476.
- [32] R. VANINBROUKX, G. BORTELS and B. DENECKE, “Alpha-particle-emission probabilities in the decay of  $^{234}\text{U}$  and photon-emission probabilities in the decays of  $^{234}\text{U}$ ,  $^{239}\text{Np}$  and  $^{243}\text{Am}$ ”, *Int. J. Appl. Radiat. Isot.*, **35** (1984) 1081-1087.
- [33] I. AHMAD, “Alpha-emitting nuclides as absolute efficiency calibration sources for germanium detectors”, *Nucl. Instrum. Meth.*, **193** (1982) 9-13.
- [34] D.I. STAROZHUKOV, YU. S. POPOV and T.A. PRIVALOVA, *Atomnaya Energia*, **42** (1977) 319.
- [35] I. AHMAD and M. WAHLGREN, “Long-lived standards for the efficiency calibration of Ge(Li) detectors”, *Nucl. Instrum. Meth.*, **99** (1972) 333-337.
- [36] V.K. MOZHAEV, V.A. DULLIN and YU.A. KAZANSKII, “Absolute measurement of the branching ratio for the 277.6-keV line of  $^{239}\text{Np}$ ”, *Atomnaya Energiya*, **47** (1979) 55-56.

- [37] L.N. YUROVA, A.V. BUSHUEV, V.I. PETROV, A.G. INIKHOV, V.N. OZERKOV and V.V. CHACHIN, “Measurement of the Absolute Intensity of the 278-keV Line of  $\text{Np}^{239}$ ”, *Atomnaya Energia*, **36** (1974) 51; *Sov. At. Energy*, **36** (1974) 52.
- [38] G.L. MOLNÁR, Zs. RÉVAY and T. BELGYA, “Non-destructive interrogation of uranium using PGAA”, IRRMA-V, Bologna, Italy, 9-14 June 2002; *Nucl. Instrum. Meth. Phys. Res.*, **B213** (2004) 389-393.
- [39] D.W. MUIR, Evaluation of correlated data using partitioned least squares: A minimum-variance derivation, *Nucl. Sci. Eng.*, **101** (1989) 88-93; NEA Data Bank, ZOTT Package-ID IAEA1371/01 (1999).

Table I

Summary of the measured 238-U thermal capture cross sections -  
standard used and quoted cross section values are listed

Lead Author	Ref.	Method	Standard material and cross section [b]	Reported cross section [b]
Anderson <i>et al</i>	[3]	Pile oscillation	<sup>nat</sup> B	703
Grumitt <i>et al</i>	[4]	Activation	<sup>55</sup> Mn	13.4
# Linenberger & Miskel	[5]	Activation	<sup>235</sup> U(f)	545
Pomerance	[6]	Pile oscillation	<sup>197</sup> Au	95
Harris <i>et al</i>	[7]	Pile oscillation	<sup>nat</sup> B	755
Egelstaff	[8]	Transmission	-	-
Crocker	[9]	Activation ( $\beta$ )	<sup>197</sup> Au	98.6 $\pm$ 0.6
Small	[10]	Pile oscillation	MnSO <sub>4</sub>	13.88 $\pm$ 0.1
Palevsky <i>et al</i>	[11]	Transmission	-	-
Cocking & Egelstaff	[12]	Transmission	<sup>197</sup> Au	98.6 $\pm$ 0.7
Egelstaff & Hall	[13]	Transmission	-	-
# Halperin <i>et al</i>	[14]	Activation	unknown	unknown
Hunt <i>et al</i>	[15]	Activation ( $\beta$ )	<sup>197</sup> Au	98.8 $\pm$ 0.3
Bigham <i>et al</i>	[16]	Activation ( $\gamma$ )	<sup>235</sup> U abs	679.9 $\pm$ 2.3
Poenitz <i>et al</i>	[17]	Activation ( $\gamma$ )	<sup>197</sup> Au	98.65 $\pm$ 0.30
De Corte & Simonits	[18]	Activation ( $\gamma$ )	<sup>197</sup> Au	98.65 $\pm$ 0.30
Rajput & MacMahon	[19]	Activation( $\gamma$ )	<sup>197</sup> Au	unknown
Molnár <i>et al</i>	[20]	Activation ( $\gamma$ )	<sup>1</sup> H	0.3326 $\pm$ 0.0007
				2.690 $\pm$ 0.045

Weighted mean of reported values = 2.705  $\pm$  0.010 barns,  $\chi^2$  per degree of freedom = 0.66.

# entries have been arbitrarily assigned 100% uncertainty.

Table II  
Measured  $k_0$  factors and derived partial cross section ratios.

$E_g [keV]$	$k_0$	<sup>a</sup> $\Delta k_0 [\%]$	$R_\gamma$	$\Delta R_\gamma [\%]$	Ref.
106.1	6.52E-03	0.6	0.007961	20.6	[25]
209.8	7.80E-04	0.5	0.000952	0.5	[18]
226+228	2.76E-03	0.7	0.003370	1.1	[25]
277.6	3.40E-03	0.8	0.004151	0.8	[18]
285.5	1.83E-04	-	0.000223	50.0	[18]
315.9	3.68E-04	1.5	0.000449	1.5	[18]
334.3	4.81E-04	1.0	0.000587	1.0	[18]

<sup>a</sup>Statistical contribution only.

Table III  
List of updated constants used in re-analysis.

Quantity	Old value	New value	Units	Ref.
$^{239}\text{U}$ decay constant	23.5	23.45	minutes	[27]
$^{239}\text{Np}$ decay constant	2.346	2.3565	days	[27]
$^{235}\text{U}/^{238}\text{U}$ abundance	0.007256	0.0072567	-	[22]
g-factor for $^{238}\text{U}$ capture	1.0017	1.0020	-	[21]
g-factor for $^{235}\text{U}$ absorption	0.9771	0.9785	-	[21]
$^{235}\text{U}$ capture to fission ratio	0.1732	0.1719 <sup>a</sup>	-	[21]
$^{235}\text{U}$ absorption cross section	679.9	683.21	barns	[1]

<sup>a</sup> Includes g-factors of 0.9910 and 0.9764 for capture and fission, respectively.

Table IV  
Beta-particle end-point energies and percentage yields from  $^{239}\text{U}$  decay.

Beta energy [keV]	$P_\beta$ [%] Old [15]	$P_\beta$ [%] New [24]
166.5	-	$0.014 \pm 0.001$
223.1	-	$0.015 \pm 0.001$
249.9	-	$0.005 \pm 0.001$
271.3	-	$0.034 \pm 0.001$
299.3	-	$0.22 \pm 0.01$
419.4	-	$0.25 \pm 0.01$
444.2	-	$0.26 \pm 0.01$
568.3	-	$0.019 \pm 0.001$
601.2	-	$0.27 \pm 0.01$
1145.8	-	$1.96 \pm 0.24$
1211	79.6	$69.0 \pm 1.4$
1232.4	-	$9.4 \pm 1.9$
1285	19.9	$18.7 \pm 2.4$

Table V  
 Summary of gamma-ray emission probability measurements  
 (expressed in %) and their absolute uncertainties.

E [keV]	Woods <i>et al</i> [31]		Vaininbroukx <i>et al</i> [32]		Ahmad [33]		Starozhukov <i>et al</i> [34]		Mozhaev <i>et al</i> [36]		Ahmad and Wahlgren [35]	
	P $\gamma$ [%]	Unc. [%]	P $\gamma$ [%]	Unc. [%]	P $\gamma$ [%]	Unc. [%]	P $\gamma$ [%]	Unc. [%]	P $\gamma$ [%]	Unc. [%]	P $\gamma$ [%]	Unc. [%]
61.6	1.4	0.07	1.29	0.02	1.29	0.06	-	-	-	-	-	-
106.1	25.23	0.28	27.5	0.4	26.4	0.8	-	-	-	-	27.8	0.9
181.7	0.085	0.005	0.07	0.01	0.083	0.004	-	-	-	-	0.083	0.004
209.8	3.43	0.07	3.46	0.05	3.3	0.1	3.36	0.14	-	-	3.42	0.1
226.4	0.230	0.014	0.28	0.02	0.290	0.016	0.24	0.03	-	-	-	-
228.2	10.91	0.16	11.21	0.18	11.2	0.3	11.78	0.48	-	-	<sup>a</sup> 11.4	0.3
254.4	0.1078	0.0027	0.12	0.01	0.11	0.006	-	-	-	-	0.11	0.01
272.6	0.0762	0.0024	0.08	0.01	0.077	0.004	-	-	-	-	0.08	0.01
277.6	14.53	0.17	14.38	0.21	14.5	0.4	15	0.5	14.3	0.24	14.5	0.4
285.5	0.797	0.01	0.77	0.02	0.79	0.025	0.93	0.06	-	-	0.76	0.02
315.9	1.604	0.02	1.6	0.3	1.6	0.05	1.63	0.07	-	-	1.52	0.05
334.3	2.05	0.025	2.08	0.03	2.06	0.06	2.1	0.1	-	-	1.95	0.07

<sup>a</sup> 228.2-keV value of Ahmad and Wahlgren [35] includes the contribution from the 226.4-keV line.

Table VI

Measured elemental partial gamma-production cross sections and derived cross section ratios.

Energy [keV]	$\sigma_\gamma$ [barns]	Uncertainty [barns]	$R_\gamma$	Uncertainty [%]
106.1	0.6567	0.0153	1.981	2.43
209.8	0.0865	0.0032	0.261	3.76
277.6	0.3888	0.0052	1.173	1.51
315.9	0.044	0.0016	0.133	3.70
334.3	0.0525	0.0044	0.158	8.41

Table VII  
Input parameters and non-informative priors for fitted parameters.

Seq. No.	Parameter	Relative Uncertainty [%]	Units	Description
1	98.65	0.091	barns	$\sigma_0(^{197}\text{Au})$
2	0.3326	0.210	barns	$\sigma_0(^1\text{H})$
3	95.58	0.126	%	$\text{Py}(^{198}\text{Au})$
4	100	0.001	%	$\text{Py}(^1\text{H})$
5	26.3	50	%	$\text{Py}(106.1 \text{ keV})$ Non-informative prior
6	0.084	50	%	$\text{Py}(181.7 \text{ keV})$
7	3.42	50	%	$\text{Py}(209.8 \text{ keV})$
8	11.4	50	%	$\text{Py}(226.4\text{--}228.1 \text{ keV})$
9	0.108	50	%	$\text{Py}(254.4 \text{ keV})$
10	0.0766	50	%	$\text{Py}(272.6 \text{ keV})$
11	14.44	50	%	$\text{Py}(277.7 \text{ keV})$
12	0.79	50	%	$\text{Py}(285.5 \text{ keV})$
13	1.6	50	%	$\text{Py}(315.9 \text{ keV})$
14	2.06	50	%	$\text{Py}(334.3 \text{ keV})$
15	2.68	50	barns	$\sigma_0(^{238}\text{U})$

Table VIII

Input data for the least squares fitting procedure. Correlated uncertainties refer to entries identified by the data sequence numbers (or their range).

Seq.No	Parameter	Rel.Unc[%]	Correlated uncertainty	Units	Description	Author	Ref.
16	2.740	2.57	17-18 0.5%	b	$\sigma_0$ (U-238)	Palevski <i>et al</i>	[11]
17	0.02714	1.5	16 0.5% ; 18 0.5%		$\sigma_0$ (U-238)/ $\sigma_0$ (Au-197)	Cocking and Egelstaff	[12]
18	2.700	1.5	16-17 0.5%	b	$\sigma_0$ (U-238)	Egelstaff and Hall	[13]
19	0.02725	1.18			$\sigma_0$ (U-238)/ $\sigma_0$ (Au-197)	Hunt <i>et al</i>	[15]
20	0.02717	0.64			$\sigma_0$ (U-238)/ $\sigma_0$ (Au-197)	Poenitz <i>et al</i>	[17]
21	0.0079606	20.6	21-27 0.5% ; 23 0.5%		R $\gamma$ (106.1 keV)	De Corte and Simonits	[18]
22	0.0009523	0.5	21-27 0.5%		R $\gamma$ (209.8 keV)	– “ –	
23	0.0033698	1.1	21-27 0.5% ; 21 0.5%		R $\gamma$ (226-228 keV)	– “ –	
24	0.0041512	0.8	21-27 0.5%		R $\gamma$ (277.6 keV)	– “ –	
25	0.0002234	50	21-27 0.5%		R $\gamma$ (285.5 keV)	– “ –	
26	0.0004493	1.5	21-27 0.5%		R $\gamma$ (315.9 keV)	– “ –	
27	0.0005873	1	21-27 0.5%		R $\gamma$ (334.3 keV)	– “ –	
28	1.981	2.43	29-32 0.5%		R $\gamma$ (106.1 keV)	Molnár and Révay	[20]
29	0.261	3.76	28 0.5% ; 30-32 0.5%		R $\gamma$ (209.8 keV)	– “ –	
30	1.173	1.51	28-29 0.5% ; 31-32 0.5%		R $\gamma$ (277.6 keV)	– “ –	
31	0.133	3.70	28-30 0.5% ; 32 0.5%		R $\gamma$ (315.9 keV)	– “ –	
32	0.158	8.41	28-31 0.5%		R $\gamma$ (334.3 keV)	– “ –	
33	25.230	1.11	34-42 1%	%	P $\gamma$ (106.1 keV)	– “ –	
34	0.085	5.88	33 1% ; 35-42 1%	%	P $\gamma$ (181.7 keV)	Woods <i>et al</i>	[31]
35	3.430	2.04	33-34 1% ; 36-42 1%	%	P $\gamma$ (209.8 keV)	– “ –	
36	11.140	1.56	33-35 1% ; 37-42 1%	%	P $\gamma$ (226-228 keV)	– “ –	
37	0.108	2.50	33-36 1% ; 38-42 1%	%	P $\gamma$ (254.4 keV)	– “ –	
38	0.076	3.15	33-37 1% ; 39-42 1%	%	P $\gamma$ (272.6 keV)	– “ –	
39	14.530	1.17	33-38 1% ; 40-42 1%	%	P $\gamma$ (277.6 keV)	– “ –	
40	0.797	1.25	33-39 1% ; 41-42 1%	%	P $\gamma$ (285.5 keV)	– “ –	
41	1.604	1.25	33-40 1% ; 42 1%	%	P $\gamma$ (315.9 keV)	– “ –	
42	2.050	1.22	33-41 1%	%	P $\gamma$ (334.3 keV)	– “ –	
43	27.500	1.45	44-52 1%	%	P $\gamma$ (106.1 keV)	Vaninbroukx <i>et al</i>	[32]
44	0.070	14.3	43 1%; 45-52 1%	%	P $\gamma$ (181.7 keV)	– “ –	
45	3.460	1.44	43-44 1% ; 46-52 1%	%	P $\gamma$ (209.8 keV)	– “ –	
46	11.490	1.74	43-45 1% ; 47-52 1%	%	P $\gamma$ (226-228 keV)	– “ –	
47	0.120	8.33	43-46 1% ; 48-52 1%	%	P $\gamma$ (254.4 keV)	– “ –	
48	0.080	12.5	43-47 1% ; 49-52 1%	%	P $\gamma$ (272.6 keV)	– “ –	
49	14.380	1.46	43-48 1% ; 50-52 1%	%	P $\gamma$ (277.6 keV)	– “ –	
50	0.770	2.60	43-49 1% ; 51-52 1%	%	P $\gamma$ (285.5 keV)	– “ –	
51	1.600	18.7	43-50 1% ; 52 1%	%	P $\gamma$ (315.9 keV)	– “ –	
52	2.080	1.44	43-51 1%	%	P $\gamma$ (334.3 keV)	– “ –	
53	26.400	3.03	54-62 1%	%	P $\gamma$ (106.1 keV)	Ahmad	[33]
54	0.083	4.82	53 1% ; 55-62 1%	%	P $\gamma$ (181.7 keV)	– “ –	
55	3.300	3.03	53-54 1% ; 56-62 1%	%	P $\gamma$ (209.8 keV)	– “ –	
56	11.490	2.75	53-55 1% ; 57-62 1%	%	P $\gamma$ (226-228 keV)	– “ –	
57	0.110	5.45	53-56 1% ; 58-62 1%	%	P $\gamma$ (254.4 keV)	– “ –	
58	0.077	5.19	53-57 1% ; 59-62 1%	%	P $\gamma$ (272.6 keV)	– “ –	
59	14.500	2.76	53-58 1% ; 60-62 1%	%	P $\gamma$ (277.6 keV)	– “ –	
60	0.790	3.16	53-59 1% ; 61-62 1%	%	P $\gamma$ (285.5 keV)	– “ –	
61	1.600	3.12	53-60 1% ; 62 1%	%	P $\gamma$ (315.9 keV)	– “ –	
62	2.060	2.91	53-61 1%	%	P $\gamma$ (334.3 keV)	– “ –	
63	27.8	23.2	64-72 1%	%	P $\gamma$ (106.1 keV)	Ahmad and Wahlgren	[35]
64	0.083	4.82	63 1% ; 65-72 1%	%	P $\gamma$ (181.7 keV)	– “ –	
65	3.42	2.92	63-64 1% ; 66-72 1%	%	P $\gamma$ (209.8 keV)	– “ –	
66	11.4	2.63	63-65 1% ; 67-72 1%	%	P $\gamma$ (226-228 keV)	– “ –	
67	0.11	9.09	63-66 1% ; 68-72 1%	%	P $\gamma$ (254.4 keV)	– “ –	
68	0.08	12.5	63-67 1% ; 69-72 1%	%	P $\gamma$ (272.6 keV)	– “ –	
69	14.5	2.76	63-68 1% ; 70-72 1%	%	P $\gamma$ (277.6 keV)	– “ –	
70	0.76	2.63	63-69 1% ; 71-72 1%	%	P $\gamma$ (285.5 keV)	– “ –	
71	1.52	3.29	63-70 1% ; 72 1%	%	P $\gamma$ (315.9 keV)	– “ –	
72	1.95	3.59	63-71 1%	%	P $\gamma$ (334.3 keV)	– “ –	
73	3.360	4.17	74-78 1%	%	P $\gamma$ (209.8 keV)	Starozhukov <i>et al</i>	[34]
74	12.020	4.24	73 1% ; 75-78 1%	%	P $\gamma$ (226-228 keV)	– “ –	
75	15.000	3.33	73-74 1% ; 76-78 1%	%	P $\gamma$ (277.6 keV)	– “ –	
76	0.930	6.45	73-75 1% ; 77-78 1%	%	P $\gamma$ (285.5 keV)	– “ –	
77	1.630	4.29	73-76 1% ; 78 1%	%	P $\gamma$ (315.9 keV)	– “ –	
78	2.100	4.76	73-77 1%	%	P $\gamma$ (334.3 keV)	– “ –	
79	14.300	1.68		%	P $\gamma$ (277.6 keV)	Mozhaev <i>et al</i>	[36]
80	37.788	3.63		%b	P $\gamma$ (277.6 keV) $\sigma_0$ (U-238)	Yurova <i>et al</i>	[37]

Table IX

Sensitivity of the fitted parameters on the removal of selected input data.  
 The uncertainties are relative uncertainties expressed as percentage of % emission probability.

	All Relative Uncertainty[%]		No De Corte Relative Uncertainty[%]		No Vaninbroukx Relative Uncertainty[%]		No Molnár Relative Uncertainty[%]		No Poenitz Relative Uncertainty[%]	
$\chi^2/\text{df}$	1.44 <sup>*</sup>		1.20		0.853		1.39		1.44	
$\sigma_0(^{238}\text{U})$	2.683	0.43	2.680	0.47	2.683	0.43	2.685	0.43	2.685	0.56
$P_\gamma(106.1)$ keV	25.34	0.7	25.48	0.7	25.25	0.7	25.41	0.7	25.33	0.7
$P_\gamma(181.7)$ keV	0.083	2.9	0.083	2.9	0.083	2.9	0.083	2.9	0.0831	2.9
$P_\gamma(209.8)$ keV	3.363	0.6	3.404	0.9	3.364	0.6	3.363	0.6	3.361	0.6
$P_\gamma(226-228)$ keV	11.50	0.8	11.32	0.9	11.50	0.8	11.50	0.8	11.49	0.8
$P_\gamma(254.4)$ keV	0.109	2	0.109	2.1	0.109	2	0.109	2	0.109	2
$P_\gamma(272.6)$ keV	0.077	2.5	0.077	2.5	0.077	2.5	0.077	2.5	0.077	2.5
$P_\gamma(277.6)$ keV	14.50	0.5	14.48	0.6	14.50	0.5	14.51	0.5	14.50	0.6
$P_\gamma(285.5)$ keV	0.794	0.8	0.794	0.8	0.793	0.8	0.795	0.8	0.794	0.8
$P_\gamma(315.9)$ keV	1.600	0.8	1.606	0.8	1.598	0.8	1.601	0.8	1.599	0.8
$P_\gamma(334.3)$ keV	2.056	0.6	2.053	0.7	2.056	0.6	2.057	0.6	2.055	0.7

All

Original analysis.

\*

Before adjustment of the outlier.

No De Corte

De Corte and Simonits data excluded entirely [18].

No Vaninbroukx

106-keV gamma-ray line of Vaninbroukx *et al* excluded from the fit [32].

No Molnár

106-keV gamma-ray line of Molnár *et al* excluded from the fit [38].

No Poenitz

Poenitz *et al* measurement excluded [17].

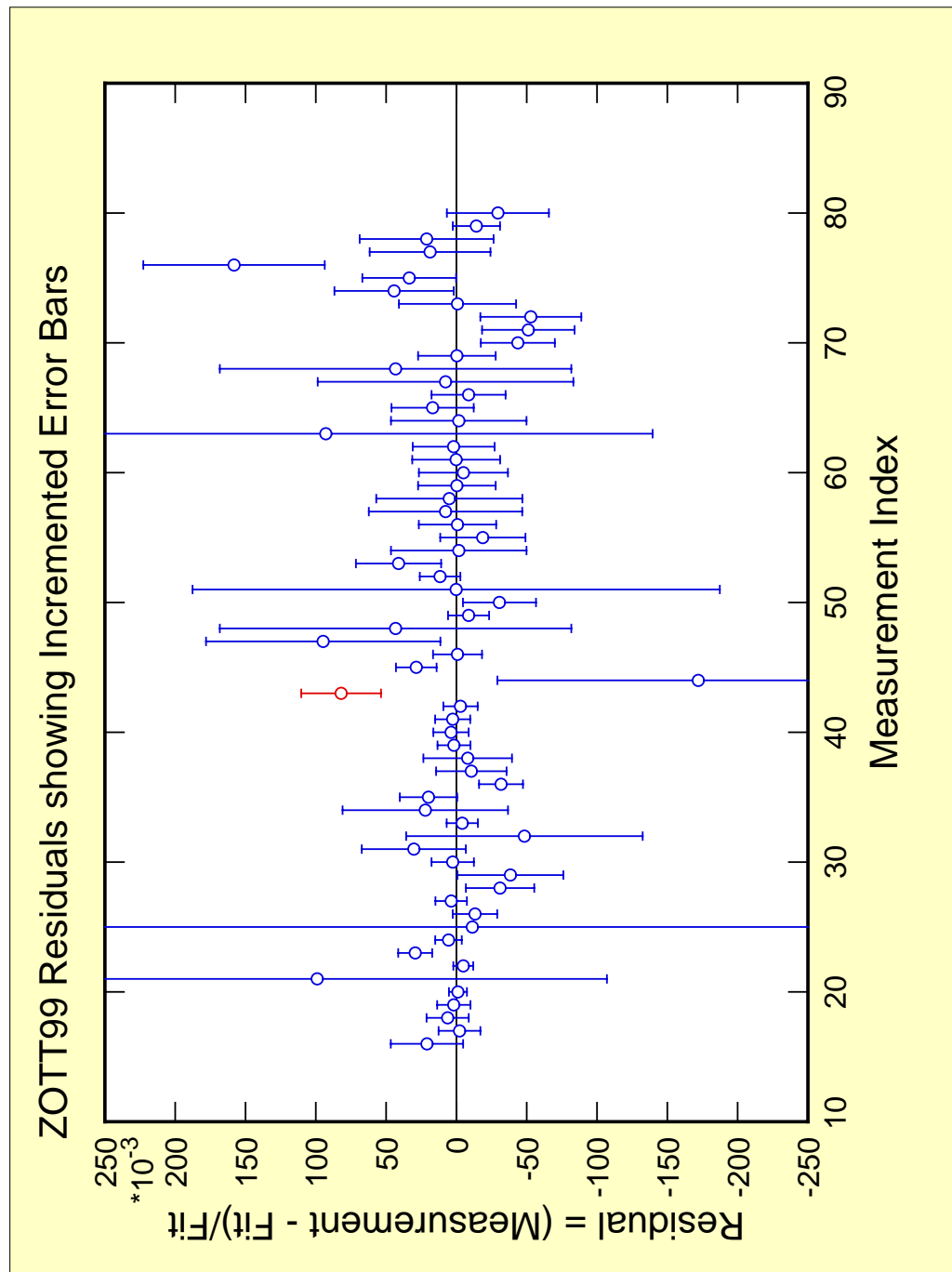


Figure 1

Relative differences of the measured data and the final fitted results. The error bars correspond to the relative uncertainties in the measured data.